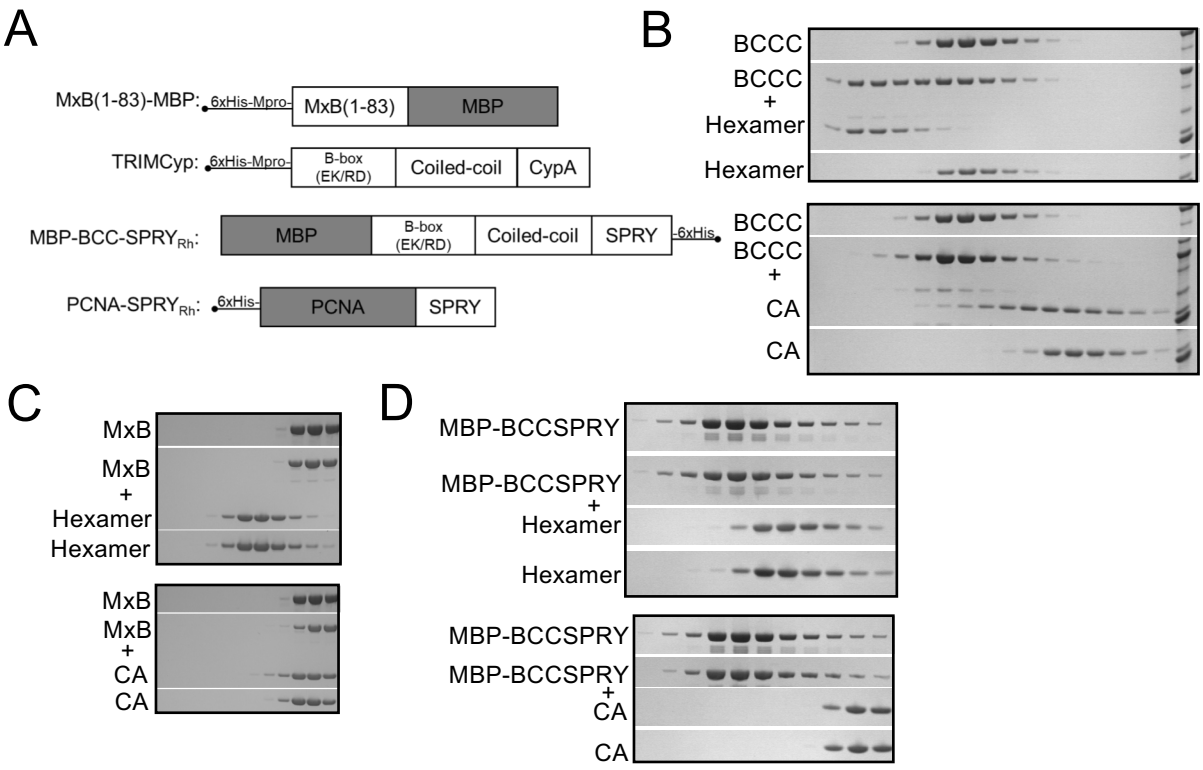

Figure S1. Related to Figure 1. Host factors demonstrate diverse CA-binding modes to established capsid assemblies. (A) Schematics of host factor constructs used in binding analysis. MBP: maltose binding protein. PCNA: proliferating cell nuclear antigen. EK/RD: E120K/R121D mutation in B-box domain to abrogate oligomerization. (B) SDS-PAGE gels from SEC coelution assays between TRIMCyp and hexamers (top) and native CA (bottom). (C) SDS-PAGE gels from SEC coelution assays between MxB(1-83)-MBP and hexamers (top) and native CA (bottom). (D) SDS-PAGE gels from SEC coelution assays between MBP-BCCSPRY$_{rh}$ and hexamers (top) and native CA (bottom).

Assembly name	CA construct #1	CA construct #2	CA construct #3
1/3-hexamer	14C/184A/185A	45C/184A/185A	
1/3-hexamer$_{EE}$	14C/42E/184A/185A	45C/54E/184A/185A	
1/3-hexamer$_{EE\text{-}mpro}$	14C/42E-Mpro-184A/185A	45C/54E/184A/185A	
1/2-hexamer	14C/184A/185A	45C/54C/184A/185A	42C/184A/185A
1/2-hexamer$_{EE}$	14C/42E/184A/185A	45C/54C/184A/185A	42C/54E/184A/185A
1/2-hexamer$_{EE\text{-}mpro}$	14C/42E-Mpro-184A/185A	45C/54C/184A/185A	42C/54E/184A/185A

Table S1. Related to Figure 2. CA constructs used in 1/3- and 1/2-hexamer assembly.

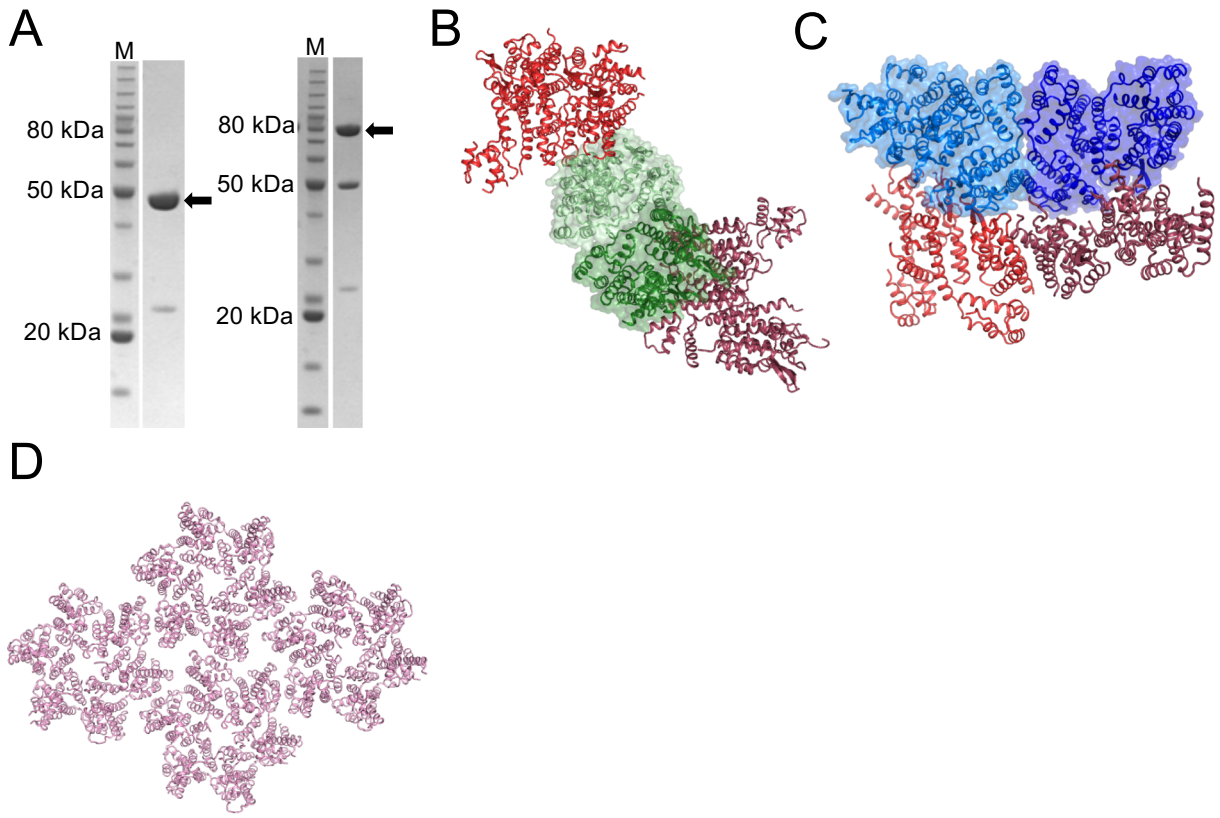

Figure S2. Related to Figure 2. Partial-hexamer assembly and structural validation. (A) Non-reducing SDS-PAGE samples demonstrating initial purity of representative 1/3- and 1/2-hexamer assemblies. Black arrows highlight the desired species that were subsequently purified. (B) Complete hexamers were not formed with applied crystal symmetry in the 1/3-hexamer$_{EE}$ crystal. The asymmetric unit contains two 1/3-hexamer$_{EE}$ assemblies (light green and green in surface representation). Symmetry mates that block hexamer formation are shown in red and raspberry. (C) Complete hexamers were not formed with applied crystal symmetry in the 1/2-hexamer$_{EE\text{-}\Delta CTD}$ crystal. The asymmetric unit contains two 1/2-hexamer$_{EE\text{-}\Delta CTD}$ assemblies (blue and marine in surface representation). Symmetry mates that block hexamer formation are shown in red and raspberry. (D) Crystal packing of the 1/2-hexamer (lacking 42E/54E mutations). In the crystal lattice 1/2-hexamers reformed complete hexamers. Each hexamer was intrinsically rotationally averaged in the crystal, thus, 1/2-hexamer divisions were not defined and individual disulfide bonds were not resolved.

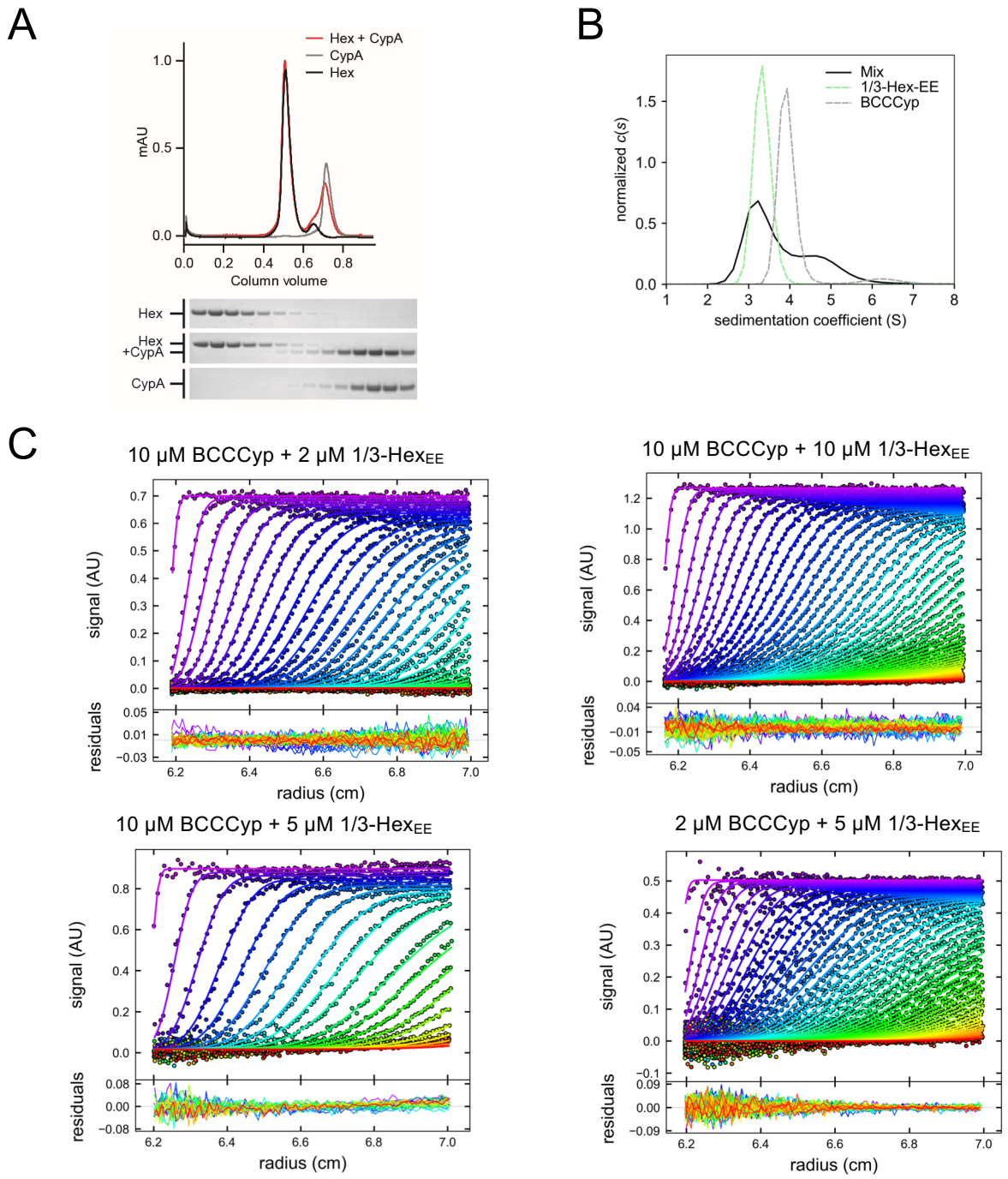

Figure S3. Related to Figure 3. Partial-hexamer assemblies reveal the flexible and avid capsid binding mode of TRIMCyp. (A) SEC coelution assay between hexamers and monomeric CypA (top). Very little coelution is observed. The corresponding SDS-PAGE of peak factions is below. (B) SV-AUC continuous distribution plots of 1/3-hexamer$_{EE}$, BCCCyp, and a mixture of 5 μM 1/3-hexamer$_{EE}$ and 2 μM BCCCyp. The mixture showed a slow-moving peak representing excess 1/3-hexamer$_{EE}$ and a fast-moving peak representing a mixture of free BCCCyp and complexed BCCCyp and 1/3-hexamer$_{EE}$. This peak is at a greater S value than that seen for BCCCyp alone, and because no peak was observed for free BCCCyp, this suggests the interaction is under fast exchange in solution relative to sedimentation. (C) SV-AUC fitted profiles after direct global Lamm Equation modeling. The RMSD values between data and fit were between 0.017 and 0.008 for the global analysis.

Assembly	**1/3-hexamer$_{EE}$**	**1/2-hexamer$_{EE\Delta CTD}$**	**Hexamer-2$_{foldon/204D1-221)}$**	**1/2-hexamer (rotationally averaged)**
Data Collection				
Wavelength (Å)	0.9798	0.9798	0.9798	0.9792
Space group	$P2_12_12_1$	$P2_12_12_1$	P321	P1
Cell dimensions				
a, b, c	74.80, 97.47, 150.89	65.60, 84.10, 248.55	95.25, 95.25, 122.57	77.77, 77.75, 77.76
α, β, γ	90, 90, 90	90, 90, 90	90, 90, 120	70.65, 70.70, 70.59
Molecules/ASU	2	3	2	6
Resolution (Å)	50.0-3.4 (3.49-3.40)	50.0-3.4 (3.49-3.40)	50.0-4.2 (4.31-4.20)	45.0-2.96 (3.01-2.96)
R_{merge}	0.14 (0.58)	0.13 (1.1)	0.11 (0.90)	0.05 (0.89)
I/σ	6.3 (1.7)	5.7 (1.0)	4.4 (1.4)	14.9 (0.90)
Completeness (%)	98.1 (99.1)	99.0 (99.1)	94.7 (89.2)	93.2 (93.8)
Redundancy	2.1 (2.1)	3.1 (3.1)	3.0 (2.6)	1.8 (1.8)
Unique reflections	15753	19697	5023	30532
CC1/2	0.985 (0.739)	0.997 (0.628)	0.997 (0.815)	(0.351)
Refinement				
# of non-hydrogen atoms	6405	8369	3252	10070
R_{work}/R_{free} (%)	21.1/27.5 (30.2/40.4)	22.5/27.5 (37.8/38.4)	28.8/31.6 (50.9/41.8)	20.5/25.3 (34.0/37.0)
Average B factor (Å^2)	76	148	191	113
Root mean-squared deviation (rmsd)				
Bond lengths	0.015	0.012	0.012	0.007
Bond angles	1.8	1.6	1.3	1.4
Ramachandran analysis				
Preferred regions (%)	96.6	96.6	96.4	93.7
Allowed regions (%)	3.1	3.0	3.4	5.2
Outliers (%)	0.3	0.4	0.2	1.2

Table S2. Related to Figure 2. Data collection and refinement statistics. Values in parenthesis are for highest resolution shell.

Assembly name	CA construct #1	CA construct #2
Tetramer-1	14C/184A/185A	45C
Tetramer-2	14C	45C/184A/185A
Tetramer-1_{EE}	14C/42E/184A/185A	45C/54E
Tetramer-2_{EE}	14C/42E	45C/54E/184A/185A
Hexamer-2	14C/42E	45C/54E
Hexamer-2_{foldon}	14C/42E	45C/54E(1-226)-foldon
Hexamer-$2_{foldon/A204D/(1-221)}$	14C/42E/204D/(1-221)	45C/54E(1-226)-foldon

Supplemental Table S3. Related to Figure 4. CA constructs used in tetramer and hexamer-2 assemblies

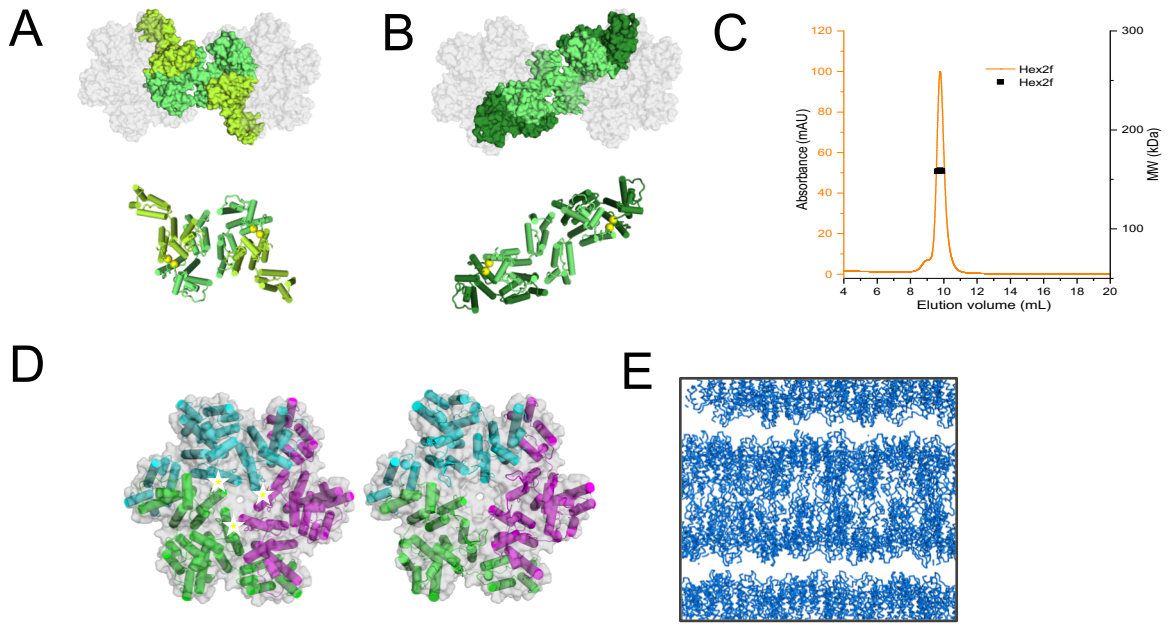

Figure S4. Related to Figure 4. Design of tetramers and assembly of hexamer-2_{foldon} containing the native 3-fold and 2-fold capsid interfaces. (A) Design of the tetramer-1 with the 14C/45C disulfide bond in yellow spheres. (B) Design of the tetramer-2 with the 14C/45C disulfide bond in yellow spheres. (C) SEC-MALS analysis of hexamer-$2_{foldon/204D/(1-221)}$ confirms it is a stable trimer. (D) Crystal packing of hexamer-$2_{foldon/204D/(1-221)}$ (right) creates a native-like capsid lattice except that traditional hexamer interfaces, indicated by stars on a native hexamer (left, a disulfide bonded hexamer from PDB ID: 3H47), are not closely packed in the hexamer-2_{foldon} crystal due to 42E/54E mutations in the hexamer-2_{foldon} design. (E) Side-view of hexamer-$2_{foldon/204D/(1-221)}$ crystal packing reveals gaps in the crystal lattice where the flexible foldon domain likely resides. Only weak, disordered foldon density is observed in these regions.

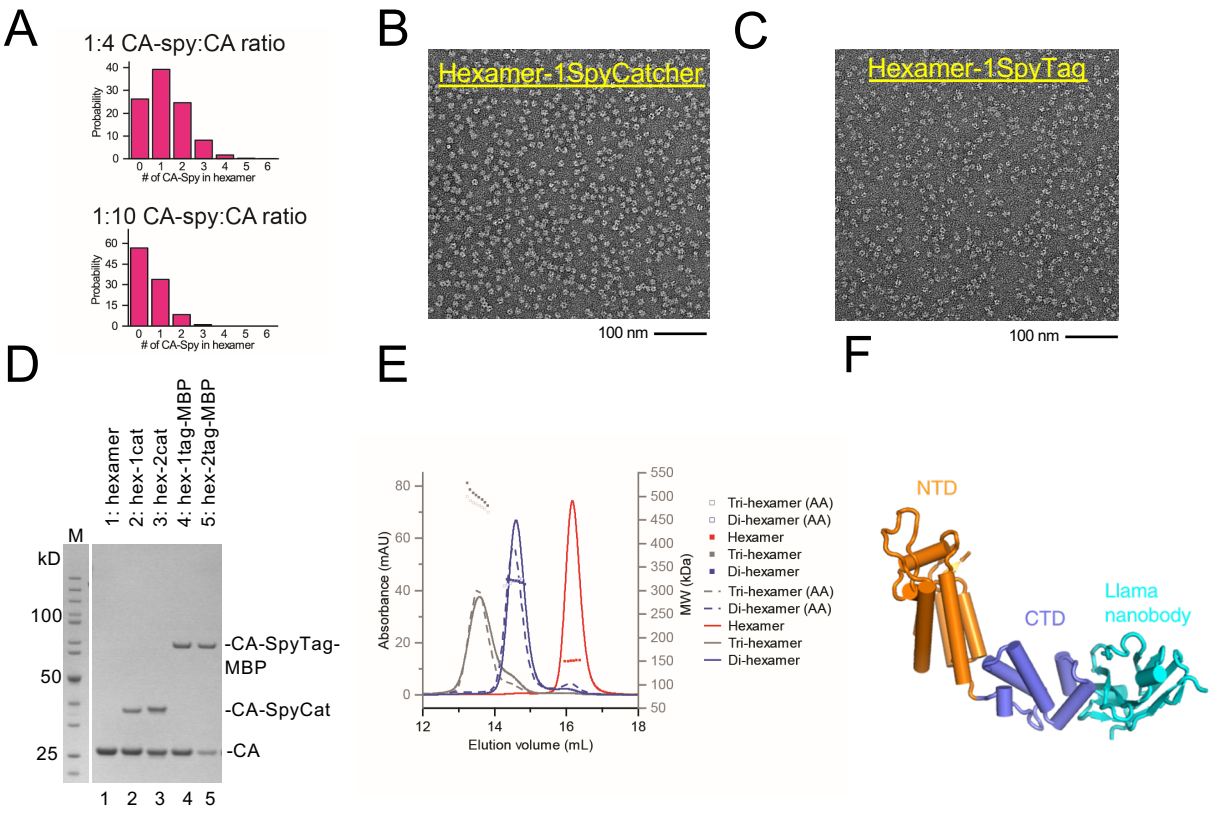

Figure S5. Related to Figure 5. Producing soluble multi-hexamer/pentamer assemblies. (A) A simple binomial distribution of the random incorporation of CA-SpyCatcher/Tag fusion into the CA hexamer. The predicted incorporation events matched what was observed experimentally. (B) Hexamer-1SpyCat is a discrete hexamer in negative-stain EM analysis. (C) Hexamer-1SpyTag is a discrete hexamer in negative-stain EM analysis. (D) Reducing SDS-PAGE samples of purified hexamers with differing CA-SpyCatcher or CA-SpyTag incorporation events. (E) SEC-MALS analysis of hexamers, di-hexamers, and tri-hexamers validates their correct solution molecular weight. (F) Model of a CA-binding nanobody in complex with a CA monomer (PDB ID: 5O2U, 3H47).

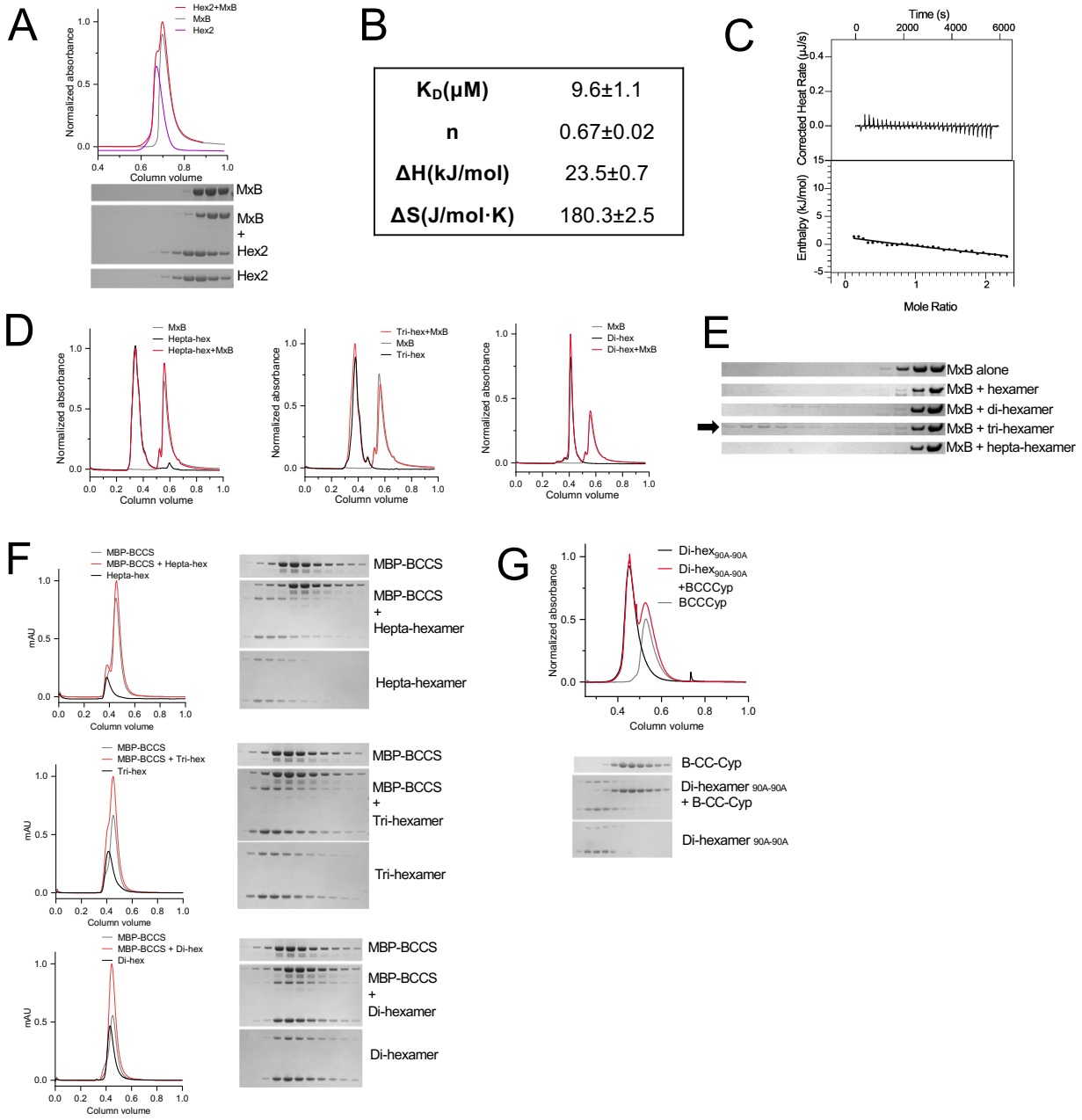

Figure S6. Related to Figure 6. MxB and TRIM5 proteins recognize inter-hexamer interfaces. (A) SEC coelution assay between MxB(1-83)-MBP and hexamer-2 without the stabilizing foldon domain. No coelution was observed. (B) Thermodynamic parameters of MxB(1-83)-MBP-hexamer-$2_{foldon/204D(1-221)}$ from triplicate isothermal titration calorimetry experiments. (C) Representative isotherm of MxB(1-83)-MBP binding to traditional hexamers using ITC. No binding curve could be fit. (D) SEC coelution assays between MxB(1-83)-MBP and hepta-hexamers, tri-hexamers, and di-hexamers. Strong coelution was not apparent from these curves. (E) SDS-PAGE samples from peaks from (D) demonstrating weak MxB(1-83)-MBP coelution with tri-hexamer assemblies indicated by black arrow. (F) SEC coelution assays between MBP-$BCCSPRY_{Rh}$ and di-hexamers, tri-hexamers, and hepta-hexamers. No coelution could be observed. Corresponding SDS-PAGE samples across peak factions are shown to the right of each chromatogram. The two bands in the hexamer assembly gels correspond to SpyCatcher-SpyTag linked CA molecules (top) and free CA (bottom). (G) Coelution assay between TRIMCyp and di-hexamers with P90A mutations at every position. No coelution was observed. Corresponding SDS-PAGE analysis is shown in the right.